Environmental Science and Pollution Research (2024) 31:54634–54647
https://doi.org/10.1007/s11356-024-34778-6

RESEARCH ARTICLE

Effect of alternative fuels on the emissions of a passenger car under real-world driving conditions: a comparison of biodiesel, gas-to-liquid, coal to liquid

Yunhua Zhang[1] · Sen Zheng[1] · Diming Lou[1] · Piqiang Tan[1] · Zhiyuan Hu[1] · Liang Fang[1]

Received: 27 March 2024 / Accepted: 18 August 2024 / Published online: 29 August 2024

Abstract

Fossil fuel energy crisis and environmental pollution have initiated the scientific research on alternative fuels. Biodiesel (B100), gas to liquid (G100), and coal to liquid (C100) are superb selections to be substitutes for conventional diesel. To better investigate the emission characteristics of the alternative fuels mentioned above, a portable emission measurement system (PEMS) was used to carry out this study under real-world driving conditions. Results showed that the driving conditions had a notable effect on the vehicle emissions, the CO, THC, and CO_2 emissions were higher under urban condition, and the NO_x, PM (particle mass), and PN (particle number) emissions were higher under suburban condition. The expressway condition resulted in lower emissions except for PN due to more nucleation particles emitted. The use of B100, G100, and C100 fuels led to a reduction of more than 50% in the CO emission, especially for the C100, but the reduction effects for the THC were not obvious, and among them, G100 is the most prominent. Higher NO_x emission was emitted after using the three fuels, especially for the B100; meanwhile, B100 increased the CO_2, but G100 and C100 decreased the CO_2 emission compared with D100. The PN emissions reduced by 1–2 orders of magnitude in comparison with those from D100 after using the three alternative fuels, and more than 50% of the PM could be reduced. B100 has the most significant particle reduction effect due to its oxygen-containing property, and it produced an evidently higher proportion of nucleation particles than D100, followed by G100 and C100.

Keywords Vehicle · Biodiesel · Gas-to-liquid · Coal to liquid · Emission characteristics · Portable emission measurement system

Introduction

Engines fueled by diesel are extensively in passenger cars because of their high working efficiency and better reliability compared to engines fueled by gasoline. What cannot be denied is that diesel engines have the overwhelming flaws of high levels of nitrogen oxide (NO_x) as well as particulate matter discharge, polluting atmosphere and environment, and doing harm to human health (Zhang et al. 2022). On the other hand, excessive consumption of fossil fuels aggravates the energy crisis and environmental pollutants (Prabhu et al. 2023; Zheng et al. 2021). In this condition, the cleaner alternative fuels are a great method to mitigate the problems mentioned above. Among the alternative fuels, the biodiesel, gas/coal to liquid are promising for their physicochemical properties. Researchers have already carried out studies about the emission characteristics of biodiesel, gas-to-liquid (GTL) fuel, and the coal to liquid. In terms of biodiesel,

Responsible Editor: Philippe Garrigues

✉ Yunhua Zhang
zhangyunhua131@tongji.edu.cn

Sen Zheng
2233576@tongji.edu.cn

Diming Lou
loudiming@tongji.edu.cn

Piqiang Tan
tpq2000@163.com

Zhiyuan Hu
huzhiyuan@tongji.edu.cn

Liang Fang
fangliang@tongji.edu.cn

[1] School of Automotive Studies, Tongji University, Shanghai 201804, China

which is considered to be one of the most prospective substitute fuels in the future by many researchers (Verma et al. 2020; Praveenkumar et al. 2023). It can be made from fatty acid methyl or ethyl esters, exhibiting different high levels of oxygen content, lower volatility, and higher viscosity in comparison with petroleum diesel. Even more remarkably, the biodiesel can be blended with petroleum diesel at any ratio, which has the potential to partially or totally replace diesel fuel (Praveenkumar et al. 2023; Zhang et al. 2023). Miao et al. (2024) conducted the Worldwide Harmonized Light Vehicles Test Cycle (WLTC) to investigate the emission characteristics of particle number (PN) of China-VI gasoline vehicles with different gasoline. They found that the gasoline with lower aromatic hydrocarbons and olefins reduced particulate matter (PM) and PN emissions by 24% and 52%, respectively. Chauhan et al. found that, with extremely lower aromatic hydrocarbon and sulfur, biodiesel generated lower SO_x as well as CO and HC emissions than diesel due to its extremely lower aromatic hydrocarbon and sulfur. But biodiesel would lead to a rise in NO_x emission compared to normal diesel fuel (Chauhan et al 2012; Verma et al. 2021a; Prabu 2018). Rao et al. (2023) found an increase in NO_x when engine speed increases; an emission reduction in NO_x was also found when they add more hydrogen fuel. Chaudhary et al. (2022) used three different kinds of biodiesel blends to test the emission characteristics, and the results showed that biodiesel blends emitted less NO_x at higher loads but caused higher NO_x emission at low loads in comparison with diesel, and a lower emission of HC and CO is followed by using biodiesel blends. Huang et al. (2020) found that the diesel blend with different alternative fuels has more oxygen content and NO_x emissions show quite a high level when biodiesel blends with alcohol at higher loads and speeds. Tian et al. (2024) found that the discrepancies of fuel-specific NOx emissions between vehicles with functioning and tampered selective catalytic reduction (SCR) systems occur mainly from medium- to high-speed modes. Tan et al. (2024) found that there was the highest CO_2 emission at the low-speed phase due to low average speed, frequent acceleration, and deceleration.

Gas to liquid fuel stands out because of its relatively low levels of gaseous and particle emissions. GTL fuel is a synthetic liquid fuel produced from natural gas via the Fischer–Tropsch process. But what is also non-ignorable can be its poly-aromatic and sulfur content. It had the benefit in soot reduction and also lower CO and NO_x emissions (Armas et al. 2013; Zhang et al. 2013; Bassiony et al. 2016). Ramos et al. (2016) found that the high cetane of GTL lead to a noticeable emission reduction in THC and CO, but only a slight decrease was found in NOx emissions in terms of using biodiesel. Soriano et al. (2018) chose biodiesel and GTL to proceed with the test under the new European driving cycle (NEDC); the reductions of the emission of THC and particles were observed, and a potential biodiesel produced by sugar fermentation was mentioned. Choi et al. (2019) found that blended biodiesel-GTL fuel resulted in reduced NO_x and soot emissions compared to those of the pure GTL fuel which is not blended with any other fuel. In the cases of HC and CO emissions, GTL-biodiesel blended fuels resulted in similar low emission trends, and, in particular, the HC emissions showed a slight increase at the range of advanced injection timings.

When it comes to coal to liquid, compared with diesel, the lower cetane number, distillation temperature, and the higher content of paraffins and naphthene are all beneficial for the homogeneous mixture formation. Different from biodiesel, the lower sulfur content, nitrogen content, and aromatics content are a good basis for nitrogen oxides and soot emissions reduction. Bin Hao et al. found the usage of coal to liquid will lead to carbonyl emissions reduction compared with ordinary diesel fuel. Coal to liquid presents a maximum percentage of about 44.1% lower ozone formation potential of the carbonyl compounds than diesel fuel under the same engine working conditions (Hao et al. 2014). Jin et al. (2018) focused on indirect and direct coal-to-liquid (ICL and DCL) and carried out their research and found that ICL did much better in soot and NO_x emissions than DCL under different conditions, indicating that ICL fuel should be an appropriate choice in cutting emissions.

What can be concluded is that scholars have extensively studied the application effects of biodiesel, gas/coal to liquid on the emission characteristics of gaseous, and particulate matter from diesel engines. However, comparative analyses among the three alternative fuels are still lack of research based on the same vehicle. On the other hand, the emission characteristics of vehicles depend on their operating conditions, which differ significantly from the emission characteristics detected by engine's test bench. The reports on the comparative studies of what the usage of biodiesel, gas to liquid GTL, and coal to liquid will do on emission characteristics based on actual vehicle operating conditions have not been released yet, thus causing a lack of a reference for quantifying the benefits of alternative clean fuels and optimizing vehicle operating conditions. Therefore, this article used a portable emission measurement system to study the emission characteristic of three alternative fuels: biodiesel, gas to liquid, and coal to liquid. Based on actual vehicle driving conditions, the emission characteristics of vehicles under different road conditions and the impact of using different alternative fuels on emission characteristics were investigated.

Experiment and methods

Test system

The test system as shown in Fig. 1 consists of an engine exhaust particle sizer spectrometer (EEPS 3090, TSI,

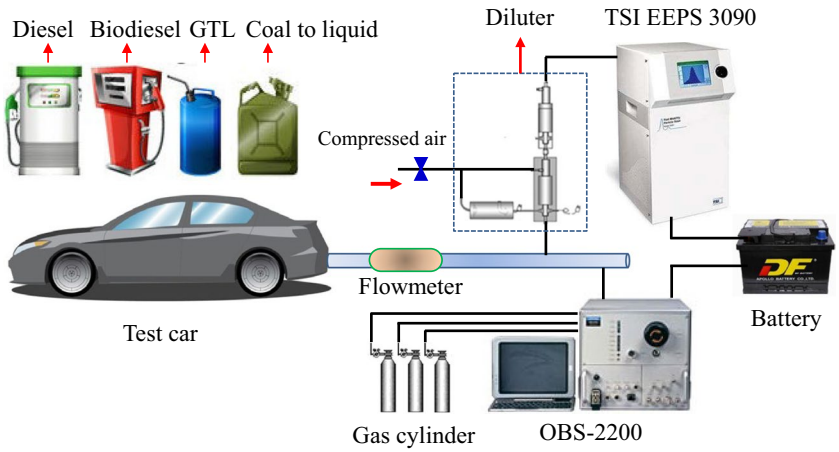

Fig. 1 Test system

USA), an on-board gaseous test device (OBS-2200, HORIBA, Japan), a two-stage diluter (DI-2000, DEKATI, Finland), a GPS, a flowmeter, and some accessories (Lou et al. 2023). The EEPS 3090 particle size analyzer can quickly measure the concentration and size distribution of particles in motor vehicle exhaust, with a measurement range of 5.6 ~ 560 nm. Within 0.1 s, a complete particle size distribution map can be obtained, and the particle number and size distribution data of 32 particle size channels can be synchronously output. The particle mass was obtained based on the particle size and particle density. The total dilution ratio is 64. The OBS-2200 is used to measure the CO, THC, NOx, and CO_2 emissions with full scales of 10%, 10000 ppm, 3000 ppm, and 20% respectively, and the testing accuracies for the four gaseous emissions are ± 2.5% full scale. The built-in program can calculate the mass emissions of the gaseous based on the volume emission concentration and flow rate. Combined with vehicle speed data, the unit mileage emissions of various gaseous pollutants of the vehicle can be further obtained. And the fuel consumptions were calculated based on the carbon balance method.

Table 1 Main specifications of the test car

Parameter	Value
Car type	SVW7193JTi
Curb weight (kg)	1435
Capacity (L)	1.9
Rated power (kW/ (r/min))	66/4000
Compression ratio	19.5
Maximum torque (N·m/ (r/min))	210/1900

Table 2 Parameters of D100, B100, G100, and C100

Parameter	D100	B100	G100	C100
Density at 20 ℃ (kg/m^3)	822	876.3	772	757
Viscosity at 20 ℃ (mm^2/s)	3.352	4.386	3.577	2.140
Freezing point (℃)	− 24	2	− 42	− 36
Sulfur content (mg/kg)	15	87	1.4	2
Low heat value (MJ/kg)	38.0	32.9	40.5	38.7
Cetane number	51.2	60.4	74.8	70
Oxygen content (%)	/	11.61	/	/
Carbon content (%)	85.50	76.26	84.56	84.26

Test vehicle

The vehicle used in the test is an in-use Passat car equipped with a TDI 1.9 L in-line four-cylinder electronically controlled pump nozzle, high-pressure direct injection turbocharged diesel engine. It has run for 21,390 km. Parameters of the car are shown in Table 1.

Test fuels

Four kinds of fuels were selected, including low-sulfur diesel (D100), biodiesel (B100), gas-to-liquid (G100), and coal-to-liquid (C100); their parameters are displayed in Table 2.

Driving conditions

The entire experiment was conducted on typical main roads in Shanghai, China. In detail, the test began on Cao'an Road in the suburb of Jiading, then proceeded through Wuning Road, Yuyao Road, and Nanpu Bridge to complete a single loop (Lou et al. 2023). The route covered 86 km and included seven subdivided road types: urban main roads, urban secondary roads, urban expressways, suburban main, secondary and expressways, and cross-river bridges. Test conditions are presented in Fig. 2. According to the calculation results, the average speeds of urban, suburban, and expressway conditions are 18.5 km/h, 29.8 km/h, and 72.3 km/h.

Main road

The main road is usually 6–8 lanes in both directions, and the capacity of the lanes should reach 1000 passenger cars units per hour. The distances between signal lights should keep not less than 800 m. In Shanghai, the main roads are divided based on regions; the main road within the Central Ring is what we described as urban main road, and the main road outside the Central Ring is what we called suburban main road. The main roads play the role of traffic trunk lines, and vehicle speed is limited to 25 ~ 30 km/h.

Secondary road

The secondary road is an inter-regional liaison trunk road within the city, which has both the functions of collecting and distributing traffic and service, and the vehicle speed on the secondary road ranges from 20 to 50 km/h. In Shanghai, the secondary road within the Central Ring is the urban secondary road, while the secondary road outside the Central Ring is the suburban secondary road.

Urban expressway

The urban expressway is a kind of road with a central dividing zone and more than four motorway lanes. All or part of the expressway adopts three-dimensional intersection to control access and exit so that the vehicle can travel at a higher speed. Expressway has a strong through-traffic characteristics, serving the long-distance fast traffic and fast external traffic in the city area. The service object of expressway is large-capacity, long-distance, and high-speed automobile traffic. Based on the goal of building modern transportation system, starting from the function of expressway, the width of red line of expressway is not less than 50 m, and the width of green isolation bandwidth is 20–50 m. The designed driving speed is generally 60–80 km/h.

Suburban expressway

Suburban expressway mainly connects urban and suburban expressways. Generally, it can adapt to 120 km/h or higher speed. It requires smooth route, small longitudinal gradient, 4–6 lane width of pavement, partition zone in the middle, asphalt concrete or cement concrete high-efficiency pavement, and tough roadbed in order to ensure traffic. Vehicle safety should be equipped with necessary signs, signals, and lighting equipment; when intersecting with railways and other highways, three-dimensional intersections should be used, and when crossing pedestrians, crossing bridges or tunnels should be used. The main difference between them and roads is that pedestrians and non-motor vehicles are forbidden to drive on the road, so they are not disturbed by other means of transportation and can ensure high-speed driving.

River-crossing bridge

The purpose of river-crossing bridge is to solve the traffic problem between rivers without obstructing the shipping of ships. It is built on the ground for the passage of people and vehicles. In order to solve the traffic problems between Pudong and Puxi, Shanghai has constructed nearly ten river-crossing bridges on the Huangpu River to promote the rapid development of the economic environment on both sides of the Huangpu River. Its design speed is generally 40 km/h.

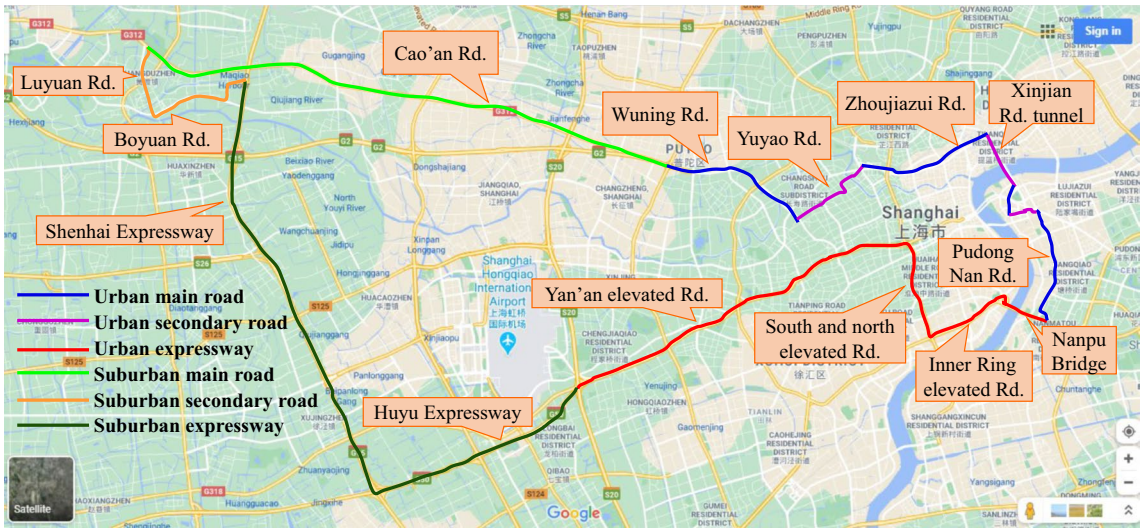

Fig. 2 Test conditions

Results and discussions

Effects of different fuels on emissions and fuel consumptions

Figure 3 shows the CO emission characteristic of vehicle fueled with D100, B100, G100, and C100 fuel under different driving conditions. The D100 produced the highest CO emission, reaching 1.19, 0.90, and 0.49 g/km under urban, suburban, and expressway conditions, respectively. When the test car was fueled with B100, the CO emission decreased significantly with a drop of more than 50%, due to the oxygen content improving the combustion. The CO emission of G100 presented a similar level as that of B100, and under suburban condition, the CO emission factor was lower than that of B100 with a decrease of 22.5%, reaching 0.41 g/km. Obviously, the CO emission factors of C100 were the lowest among the four fuels, especially at urban condition, which decreased by more than 35% compared with G100. The CO emission factor of C100 at expressway was the lowest, reaching only 0.22 g/km; this is because C100 has a low viscosity and high cetane number, which is beneficial to the atomization and combustion of the fuel (Işik 2021).

Figure 4 shows the CO_2 emission characteristic of vehicle fueled with D100, B100, G100, and C100 fuel under different driving conditions. Under the urban and suburban conditions, B100 produced the highest CO_2 emission factors, reaching 203.27 and 202.25 g/km, followed by those of D100 and C100, and the CO_2 emission factors of G100 were the lowest, reaching 177.63 and 121.45 g/km, respectively, under the two driving conditions. The reason for the high CO_2 emission using biodiesel is the low heat value, causing a high fuel consumption (Gundoshmian et al. 2021; Verma et al. 2021b). When the test car was operated under expressway condition, the CO_2 emission factors were the lowest, and the effects of fuels on the CO_2 emission factors were different from the previous two driving conditions; in detail, the D100 produced the highest CO_2 emission factor, followed by that of B100, which are 138.42 and 129.51 g/km, respectively, and CO_2 emission factors of G100 and C100 were similar with a value of about 121 g/km.

Figure 5 shows the THC emission characteristic of vehicle fueled with D100, B100, G100, and C100 fuel under different driving conditions. In general, THC emissions of different fuels under expressway condition were the lowest, while for the urban and suburban conditions, their emissions had little difference. When the test vehicle operated under urban condition, the THC emission of D100 was the highest with a value of 0.043 g/km, followed by those of B100, C100, and G100, with THC emission factors of 0.040, 0.036, and 0.030 g/km, respectively. When the test vehicle operated under the suburban condition, the THC emission of B100 was the highest, with a value of 0.054 g/km, while the THC emission of G100 was only 0.028 g/km, and for D100 and C100, their THC emission factors were about 0.039 g/km. When the test vehicle operated under the expressway condition, the THC emissions of B100 and G100 were similar with a value of 0.017 g/km. The revealed high THC emission results in the urban area may associate with the passenger car traffic (Yang et al. 2019).

Figure 6 shows the NO_x emission characteristic of vehicle fueled with D100, B100, G100, and C100 fuel under different driving conditions. The NO_x emissions were at the same level when the vehicle was driving on different conditions. When the vehicle was operated under urban condition, the NO_x emission factor of B100 was the highest, which shows a value of 1.40 g/km; the NO_x emissions of C100, G100, and D100 decreased sequentially, with values of 1.23, 1.19,

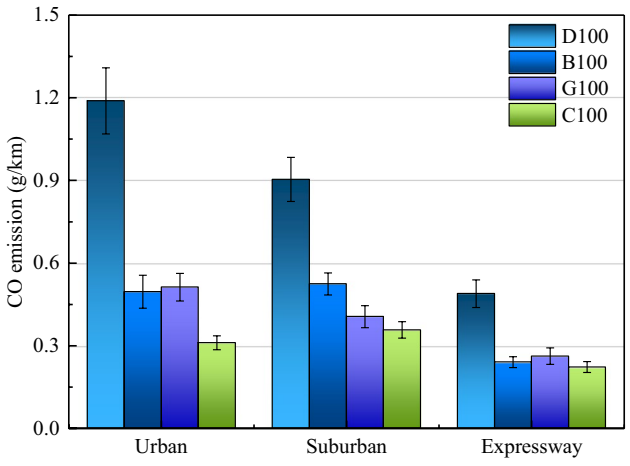

Fig. 3 CO emissions of vehicle fueled with D100, B100, G100, and C100

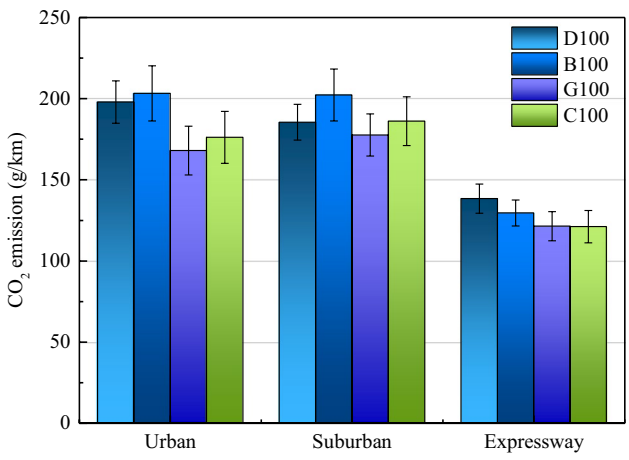

Fig. 4 CO_2 emissions of vehicle fueled with D100, B100, G100, and C100

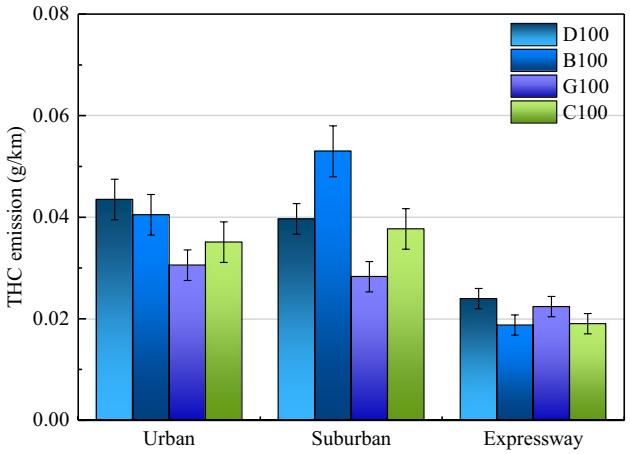

Fig. 5 THC emissions of vehicle fueled with D100, B100, G100, and C100

and 1.07 g/km, respectively. Under suburban conditions, B100 still had the highest NO_x emissions with a value of 1.42 g/km, while G100 had a value of 1.40 g/km, and C100 and D100 had similar emissions of 1.24 g/km and 1.21 g/km, respectively. The NO_x emission factors, which are easy to be observed between different working conditions, decrease as the vehicle speed increases (Wei et al. 2020). Under highway conditions, B100 also had the highest NO_x emission with a value of 1.22 g/km, while the NO_x emission of G100 was similar, reaching 1.21 g/km. In terms of D100 and C100, their NO_x emission factors were 1.05 and 0.99 g/km, respectively.

Figure 7 shows the particle mass (PM) emission characteristic of vehicle fueled with D100, B100, G100, and C100 fuel under different driving conditions. Apparently, the PM emission factor of D100 was the highest among the four fuels. When the vehicle was fueled with B100 under urban condition, the PM emission decreased significantly, and B100 led to a drop of 37.4% in the PM emission compared with D100, and under suburban and expressway conditions, the drops further enlarged. The gas to liquid, a volatile fuel, is beneficial for generating mixed gas, contributing to reduce particulate emission (Alves et al. 2023). When the vehicle was fueled with G100, the PM emission further decreased; under the urban, suburban, and expressway conditions, the drops reached 50.3%, 58.5%, and 60.3%, respectively. The C100 fuel led to a similar reduction effect on the PM emission as B100; under the urban, suburban, and expressway conditions, the reductions were 45.8%, 46.5%, and 49.4%, respectively. From the view of reducing PM, the G100 was the best, followed by the C100 and B100.

Figure 8 shows the particle number (PN) emission characteristic of vehicle fueled with D100, B100, G100, and C100 fuel under different driving conditions. Due to the low kinematic viscosity and high cetane of G100 and C100, it can improve fuel's atomization and combustion abilities, thus reducing PN emissions (Mei et al. 2020). B100's low PN emission can be attributed to its oxygen content, aromatics, and cetane number. When using D100 fuel, the PN emission factor of the vehicle reached 1.47×10^{15} particles/km under urban operating conditions, whose PN was the same under expressway condition. The PN emission factor decreased to 1.26×10^{15} particles/km under the suburban operating conditions. When using B100, G100, and C100, the PN emission factors declined significantly. For B100, the PN emission factors under urban, suburban, and expressway conditions showed a similar reduction rate of 71.9%, 75.0%, and 72.4%, respectively. For G100, the PN emission factors under urban and expressway conditions were further reduced compared to B100, while the PN emission factor under suburban condition increased slightly. The PN emission reduction rates

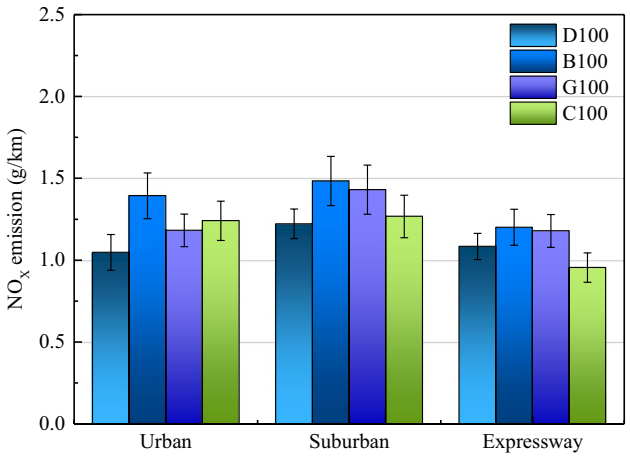

Fig. 6 NO_x emissions of vehicle fueled with D100, B100, G100, and C100

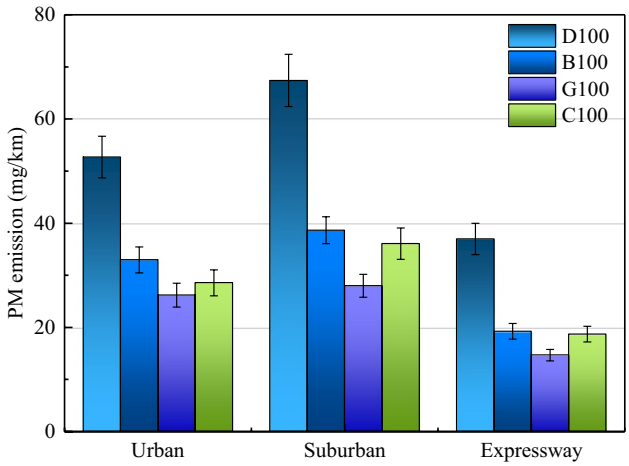

Fig. 7 PM emissions of vehicle fueled with D100, B100, G100, and C100

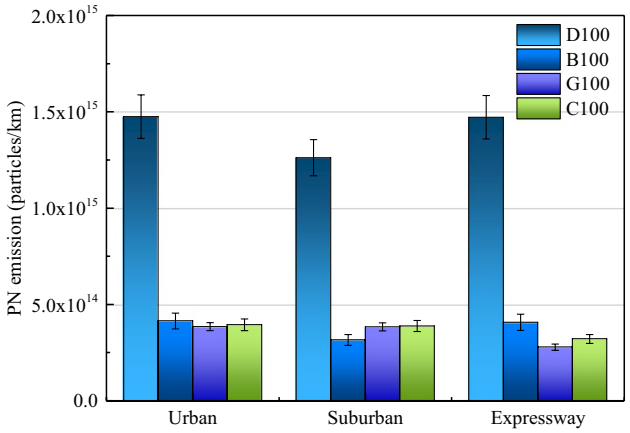

Fig. 8 PN emissions of vehicle fueled with D100, B100, G100, and C100

under the three operating conditions were 73.9%, 69.6%, and 81.1%, respectively. The PN emission factor of C100 was equivalent to G100; in addition, it showed a reduction rate of 73.2%, 69.3%, and 78.2% under urban, suburban, and expressway conditions, respectively. Higher cetane number fuels ignite faster and more completely, leading to improved combustion efficiency, reduced ignition delay, smoother engine operation, and lower emissions (Yuan et al. 2022).

Figure 9 shows the particle size distribution characteristics of particulate emissions from vehicle fueled with D100, B100, G100, and C100 fuel under different driving conditions. For particles from G100 and C100, their main components were linear chain saturated hydrocarbons, which caused an easier cracking during combustion, thus generating smaller-size particles (Alsudani et al. 2023). When using D100, peak points in both nucleation and accumulation modes were observed at 9.31 nm and 165.5 nm corresponding to particle size. And the accumulation mode particles of D100 were larger than those of other fuels. Under urban conditions, in terms of nucleation mode particulates' region, the average particle sizes using B100 and D100 were slightly larger than those using G100 and C100. In the accumulation mode particulates' region, the average particle sizes using C100 were slightly larger than those using G100 and C100, while the particle sizes distribution of G100 and B100 were roughly the same. Under suburban conditions, in the nucleation mode particulates' region, the average particle sizes when using B100 and D100 are slightly larger than those using G100 and C100. When using C100, G100, and B100, in the accumulation mode particulates' area, the average particle sizes decreased sequentially. Under urban conditions, in the nucleation mode particulates' region, the average particle sizes using B100 were slightly larger than those using G100, B100, and C100. When using C100, G100, and B100, in the accumulation mode particulates' area, the average particle sizes decreased sequentially, but the difference between the three was slightly greater than that of the suburban conditions.

Figure 10 shows the particle proportions characteristics of the test car when using D100, B100, G100, and C100 under different working conditions. Obviously, the total particulate emission of D100 was much higher than that from the other three fuels. For B100, its abundant oxygen in molecule promoted the transformation of large-size soot particles into small-size soot particles, resulting in a number increase of nucleation mode particles (Tong et al. 2021). For G100 and C100, the low content of aromatic hydrocarbons reduces the high-temperature cracking components in the combustion process, which fundamentally suppressed the formation of accumulated particles (Ahmad et al. 2021). In addition, when using the same fuel, accumulated-mode particles had a proportion of around 87%. For the other three fuels, under urban and suburban conditions, the proportion of accumulated-mode particles was higher than nuclear-mode particles, and total particle emission brought by using B100, G100, and C100 declined by approximately 67%. Under expressway condition, the number of nuclear-mode particles was higher than accumulated-mode when using B100 and G100, and the total particulate emission brought by using B100, G100, and C100 declined by approximately 75%.

Figure 11 shows fuel consumption using D100, B100, G100, and C100 under urban, suburban, and expressway conditions. Under expressway condition, the fuel consumption is lower than that in urban and suburban conditions, and the difference in fuel consumption was not visible between fuel types. Under urban and suburban conditions, the fuel consumption of B100 reaches 8.34 L/100 km under urban condition and 8.57 L/100 km under suburban condition, respectively. Average fuel consumption for D100, B100, G100, and C100 under urban, suburban, and expressway situations were 6.74 L/100 km, 7.41 L/100 km, 6.54 L/100 km, and 6.72 L/100 km, respectively. The average fuel consumption of B100 was 12.6% higher than of D100, and the fuel consumptions of G100 and C100 kept a roughly equivalent level as D100.

Effects of running conditions on vehicle emissions

In order to study the effects of running conditions on the emissions, the D100 was chosen as a baseline to investigate the emissions of the test vehicle under different running conditions.

Figure 12 shows the proportion of vehicle operating conditions under different road conditions. In urban main road, the proportion of constant speed condition was the largest, reaching 36.0%, followed by the idling condition, with a proportion of 31%. The proportion of acceleration and deceleration condition was similar. For the urban secondary road

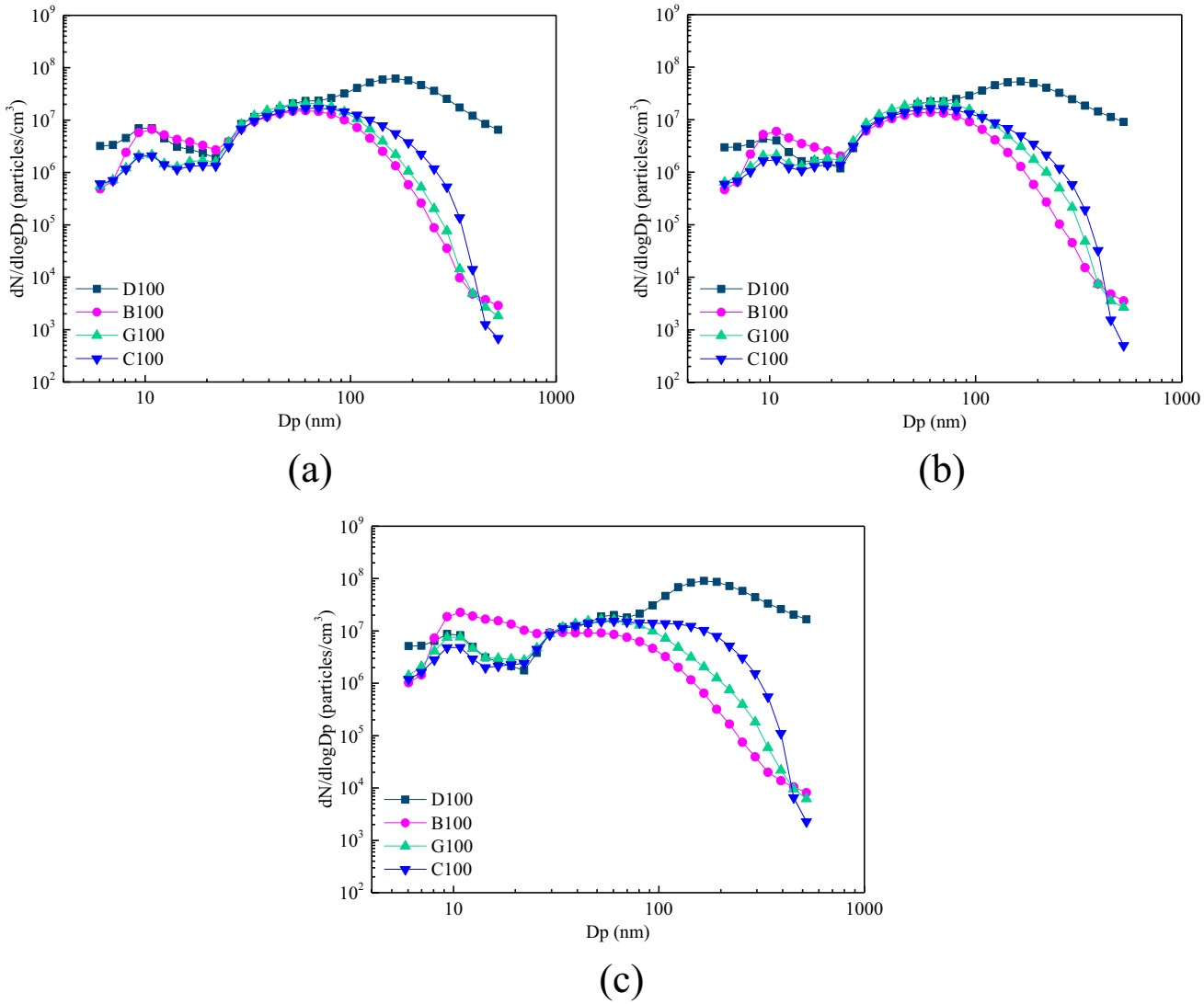

Fig. 9 Particle size distribution characteristics of vehicle fueled with D100, B100, G100, and C100: **a** urban condition, **b** suburban condition, and **c** expressway condition

and urban expressway condition, the proportion of idling condition decreased remarkably, with a drop of 19.0% and 0.9%, respectively, while the acceleration and deceleration condition proportions increased. Especially for the urban expressway condition, the proportions of acceleration and deceleration condition exceeded 40%. The changes of the proportions of driving conditions in suburban condition were the same as those in urban main road. For river crossing bridges driving condition, the acceleration and deceleration conditions accounted for more than 40%, and the idling conditions accounted for only 0.3%.

Figure 13 shows the CO emission characteristics of vehicle using D100 under different driving conditions. The maximum CO emission value that appeared in the urban main road condition was 1.46 g/km. This may be due to the high proportion of acceleration sections in urban road conditions, and low air-to-fuel ratio can increase HC emissions of engine (Koay et al. 2019). When the vehicle was operated on urban secondary road and expressway, it could be observed that the emissions of CO reduced sequentially with a value of 1.27 and 0.83 g/km, respectively. In terms of CO emission in suburban condition, a downward trend was observed compared with those in urban condition. The maximum CO emission appeared in the suburban main road condition, reaching 0.99 g/km, with a drop of 32.2% in comparison with that at urban main road condition. When the test vehicle operated in the river-crossing situation, emission factor of CO was comparatively low with a value of 0.50 g/km. The main reason is that under the main road condition, there are many pedestrians, motor vehicles, intersections,

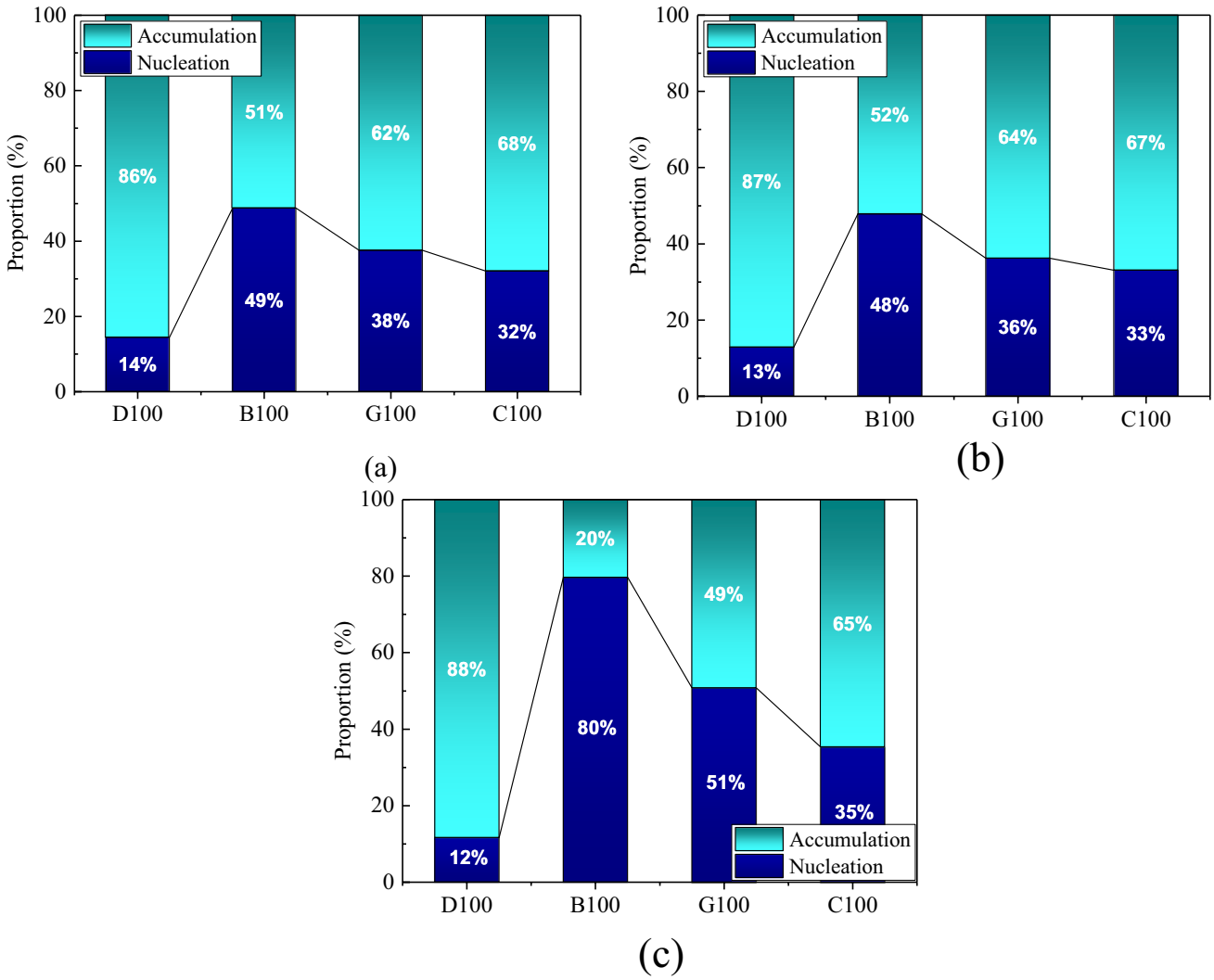

Fig. 10 Particle proportions characteristics of vehicle fueled with D100, B100, G100, and C100: **a** urban condition, **b** suburban condition, and **c** expressway condition

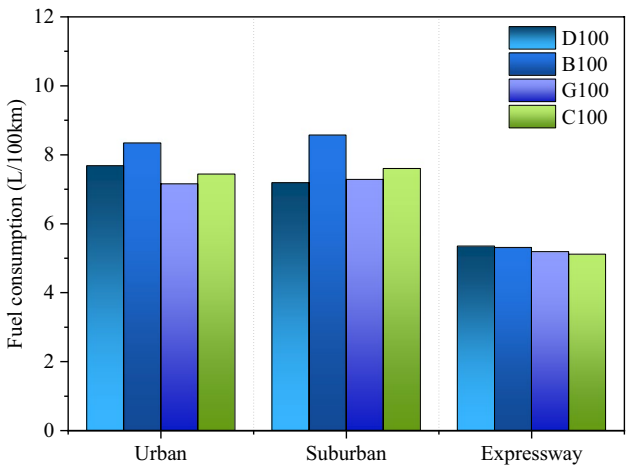

Fig. 11 Fuel consumption using D100, B100, G100, and C100 under different driving conditions

and traffic lights, causing a high proportion of idle condition of the vehicle, in which the in-cylinder temperature is low, and fuel combustion is incomplete, leading to an increase in CO emission (Ge et al. 2022). When the vehicle operated on the urban secondary road, the proportion of idle condition declines, and the combustion of the fuel improved, producing a reduction in the CO emission. When the vehicle operated on the urban expressway condition, the vehicle engine was in a stable and high-efficiency condition, and the fuel combustion was more complete, causing a low CO emission (García et al. 2019). On the suburban road, the CO changing trend is attributed to the same reason.

Figure 14 shows the THC emission characteristics of vehicle using D100 under different driving conditions. The emission factor under urban main road condition was the highest, reaching 0.056 g/km, and a decreasing trend can be observed in the THC emission factors from suburban

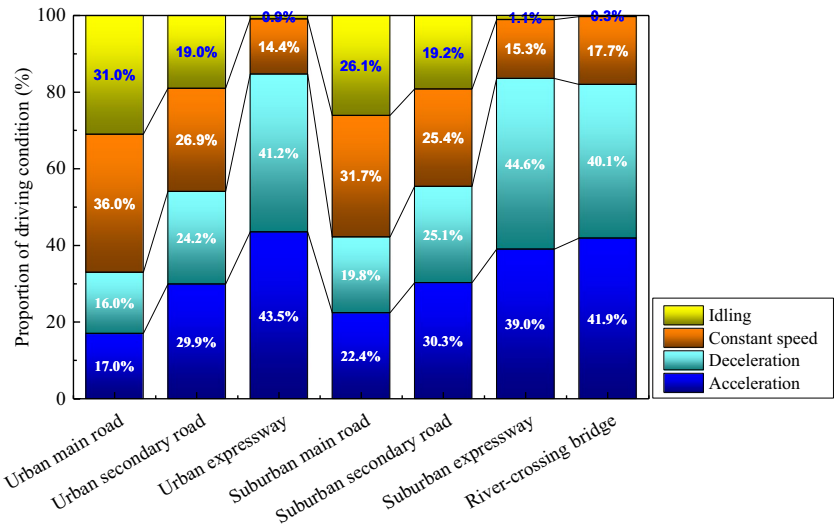

Fig. 12 The proportion of vehicle operating conditions under different road conditions

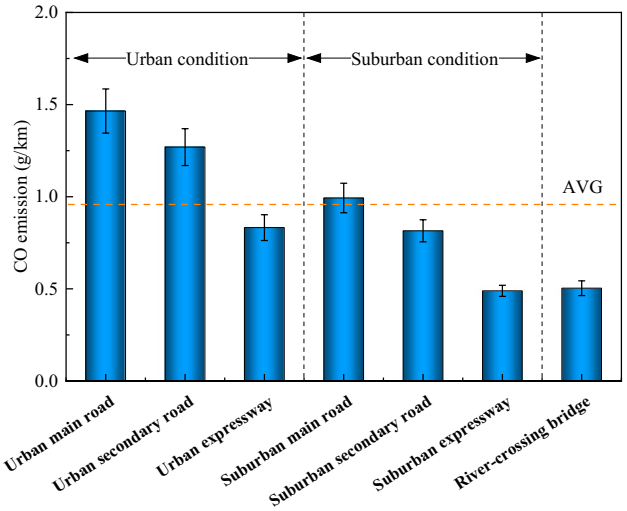

Fig. 13 CO emissions of the test car using D100 under different driving conditions

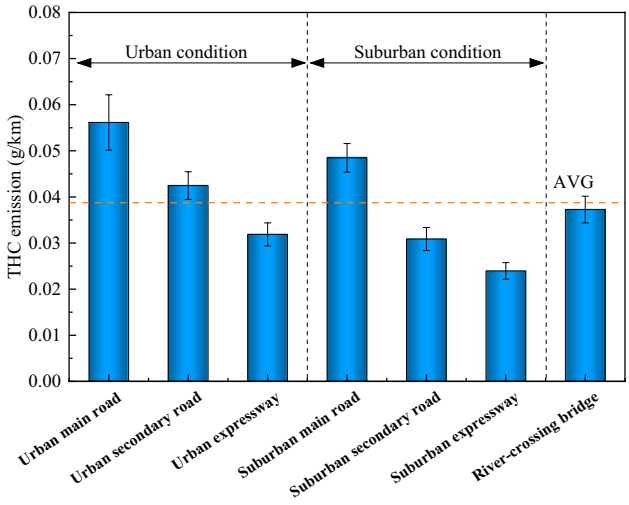

Fig. 14 THC emissions of the test car using D100 under different driving conditions

condition to expressway condition. The excess air ratio, which has a significant impact on THC emission, changes frequently during idling period, causing an increase in THC emission (Zhao et al. 2013). The THC emission factors under suburban conditions were lower than those under urban condition, and the THC factors were 0.048, 0.031, and 0.024 g/km, respectively. Notably, the THC emission factor increased slightly with a value of 0.037 g/km under river-crossing bridge condition. The changing trend of the THC emission with the operating condition was similar to that of CO emission.

Figure 15 shows the NO_x emission characteristics of vehicle using D100 under different driving conditions. Obviously, the NO_x emissions were at the same level at urban and suburban conditions. When the vehicle operated on the urban main and secondary road, the NO_x emission factors were 1.16 and 1.14 g/km, respectively. When the test vehicle operated on the urban expressway, the NO_x emission factor decreased slightly to 0.84 g/km due to higher average vehicle speed. The NO_x emission factors on suburban road condition were still high, reaching 1.16 g/km, 1.29 g/km, and 1.08 g/km on suburban main road, secondary road, and expressway, respectively. When the test vehicle operated on the river-crossing bridge condition, the NO_x emission factors declined remarkably to 0.62 g/km. Among them all, it can be seen that the NO_x emission exhibited a low level under urban expressway and river-crossing bridge condition. The main reason may lie in the idling stage; engine's torsion can change quickly. When the vehicle accelerates too often, it will cause a high temperature and a rich diesel mixture in

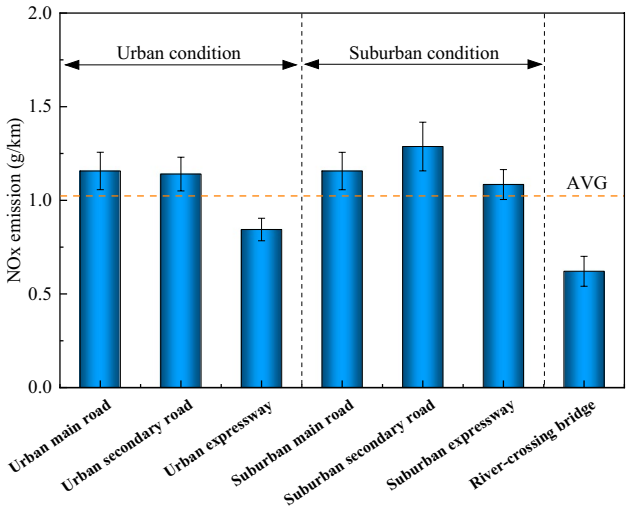

Fig. 15 NO_x emissions of the test car using D100 under different driving conditions

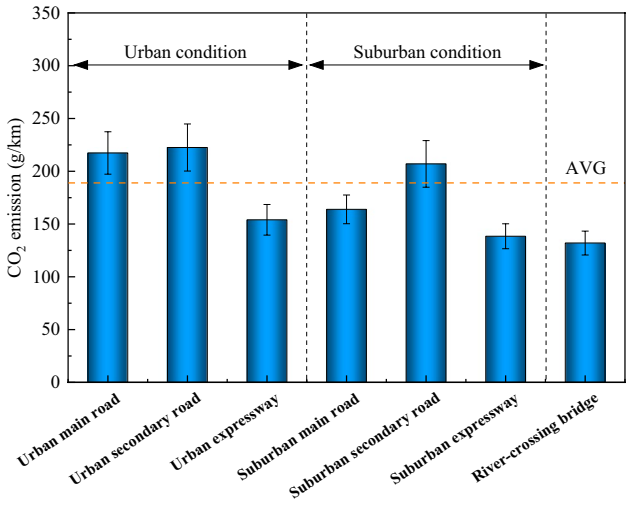

Fig. 16 CO_2 emissions of the test car using D100 under different driving conditions

engine's cylinder, thus causing a high NO_x emission (Gao et al. 2021). When the test vehicle accelerates, the engine advances the diesel injection timing and quantity in order to quickly change power, which leads to an increase in NO_x (Ravaglioli and Bussi 2019). Low air-to-fuel ratio can reduce NO_x emissions. Concentrated mixtures are typically used in acceleration conditions to increase power output, resulting in lower fuel consumption, which helps improve fuel economy, but may lead to insufficient power output.

Figure 16 gives the CO_2 emission characteristics of vehicle using D100 under different driving conditions. The CO_2 emission factors changing trend with the conditions were consistent with that of NO_x. When the test vehicle operated on the urban main road and secondary road, the CO_2 emission factors were 217.31 g/km and 222.48 g/km, respectively, keeping a high level due to a large proportion of idling condition needing more fuel (Kim et al. 2018). When the vehicle was operating on urban expressway, the CO_2 emission factor declined to 154.01 g/km. For suburban main and secondary road, the CO_2 emission factors were 163.92 g/km and 207.10 g/km, respectively. When the test vehicle operated on the river-crossing bridge condition, the CO_2 emission factor was 132 g/km, which is only 59.3% of the CO_2 emission on the urban secondary road.

Figure 17 shows the PN emission characteristics of vehicle using D100 under different driving conditions. The PN emission under urban condition and suburban condition showed great difference. For the urban condition, the PN emissions were roughly the same. In detail, the PN emission factors were 1.38×10^{15} particles/km, 1.54×10^{15} particles/km, and 1.51×10^{15} particles/km, respectively. During the suburban condition, the PN emissions fluctuated greatly. The PN emission factor on the suburban road was very low with a value of 4.3×10^{14} particles/km; this is because the suburban road is wide, there was less traffic flow, the proportion of acceleration and deceleration condition is higher, and the fuel burning is more complete; the particles were further fully oxidized (Tang et al. 2022). But for the suburban secondary road and expressway, a higher speed of the vehicle and improved fuel combustion causing more fine particles resulted in a higher PN emission factor. When the test vehicle operated on the river-crossing bridge, the PN emission reached maximum with a value of 2.14×10^{15} particles/km.

Figure 18 shows the PM emission characteristics vehicle using D100 under different driving conditions. The PM emission factors on urban main and secondary road were almost the same, reaching 59.38 mg/km and 58.29 mg/

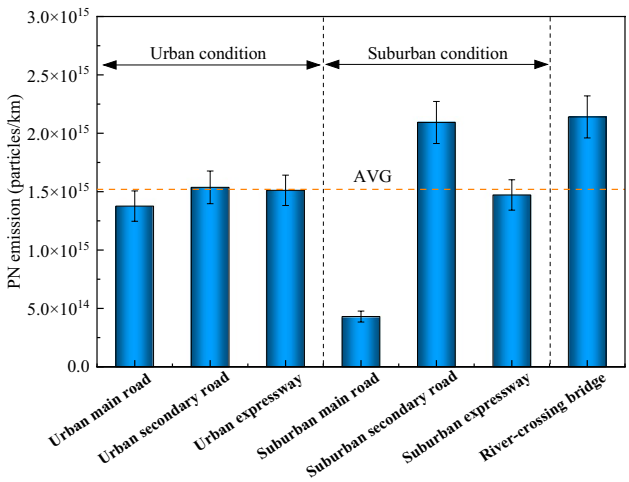

Fig. 17 PN emissions of the test car using D100 under different driving conditions

km, respectively. While the PM emission factor on urban expressway declined obviously, with a value of 40.38 mg/km, this is because the vehicle had a higher speed and a stable operation state at this condition, improving the combustion of the fuel and oxidation of the particles (Lü et al. 2020). During the suburban condition, the PM emission factors changed drastically. For suburban main road, the PM emission factor was very closed to the average value during the whole test. When the test vehicle operated on suburban secondary road, the emission of PM increased sharply due to more fine particles were emitted (Verma et al. 2019). For the suburban expressway, a higher vehicle speed caused the PM emission presented a declining trend, with a value of 37.0 mg/km. When the test vehicle operated on the river-crossing bridge condition, the PM emission factor further declined to 33.49 mg/km.

Figure 19 shows the particle size distribution (PSD) characteristics of vehicle using D100 under different driving conditions. The PSD basically presented a two-peak distribution at 10.8 nm and 165.5 nm. Nucleation mode particles are exhaust particles with a particle size of 5–50 nm, and accumulation mode particles are particles with particle size larger than 50 nm. Most of the particles are in the 10–100 nm class (Liu and Tan 2020). In terms of the peaks at nucleation mode particles, they were higher under urban expressway and suburban expressway conditions (Joerger and Pryor 2018), and the peaks under urban main road and suburban main road conditions were lower than other conditions. For the peaks at accumulation mode particles, it showed the highest level under river-crossing bridge condition, followed by urban expressway and suburban expressway conditions (Krecl et al. 2017), and peaks at urban secondary road and urban main road conditions were the lowest. Notably, the peak under suburban main road condition at accumulation mode particles appeared at 80.6 nm, smaller than other driving conditions.

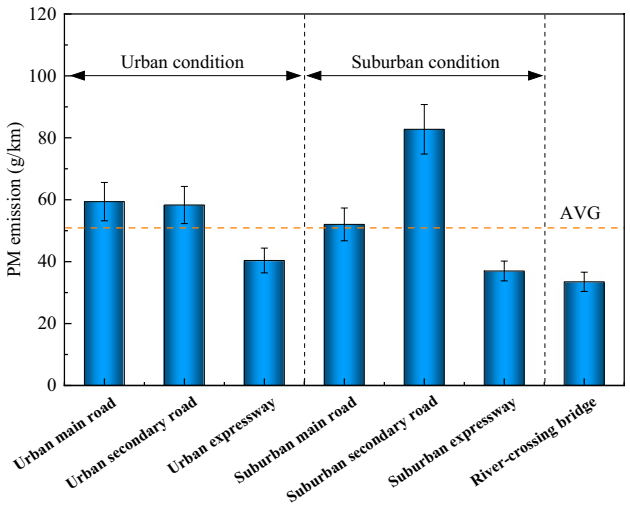

Fig. 18 PM emissions of the test car using D100 under different driving conditions

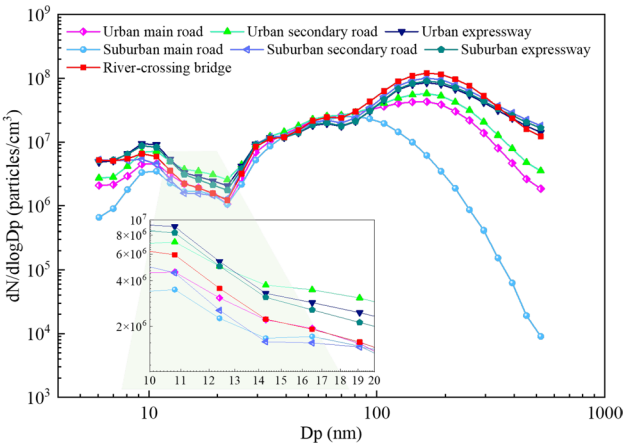

Fig. 19 Particle size distribution of the test car using D100 under different driving conditions

Conclusions

In this study, a PEMS method was used to investigate the emissions of a vehicle fueled with diesel, biodiesel, GTL, and coal to liquid under real-world driving conditions. The main conclusions are as follows.

(1) The emissions of the test vehicle depended on the driving conditions. The CO, CO_2, and THC emissions were higher under urban condition, and the NO_x, PM, and PN emissions were higher under suburban condition. The expressway condition resulted in lower emissions except for PN emission due to more nucleation particles were emitted.

(2) The use of B100, G100, and C100 fuels led to a reduction of more than 50% in the CO emission, especially for the C100. In terms of the THC reduction effect, the use of B100, G100, and C100 was not obvious. Higher NO_x emission was emitted after using the three fuels, especially for the B100, which produced the highest NO_x emission factor with a value of 1.49 g/km under suburban condition, and resulted in a higher CO_2 emission; also, the fuel consumption of B100 was the highest.

(3) The use of the three alternative fuels reduced the PN emissions by 1–2 orders of magnitude compared with D100, and more than 50% of the PM could be reduced; B100 performed better among the three fuels in reducing particle emissions. But it produced a significantly higher proportion of nucleation particles than D100, followed by G100 and C100.

Nomenclature CO: Carbon monoxide; CO_2: Carbon dioxide; THC: Total hydrocarbons; HC: Hydrocarbon; NO_x: Nitrogen oxides; PM: Particulate matter; PN: Particulate number; SO_x: Sulfur oxides; B100: Pure biodiesel fuel; C100: Pure coal to liquid fuel; G100: Pure gas to liquid fuel; D100: Pure diesel fuel; GTL: Gas to liquid fuel; PEMS: Portable emission measurement system; TDI: Direct injection diesel engine; PSD: Particle size distribution

Author contribution Yunhua Zhang: conceptualization, methodology, writing—review and editing.

Sen Zheng: formal analysis, writing—original draft, data curation, software.

Diming Lou: resources, investigation, project administration.

Piqiang Tan: supervision, project administration.

Zhiyuan Hu: resources, project administration.

Liang Fang: supervision, resources.

Funding This study was supported by the National Natural Science Foundation of China (52206167) and the Fundamental Research Funds for the Central Universities (No. 22120220582).

Data availability The datasets generated and supporting the findings of this article are obtainable from the corresponding author upon reasonable request.

Declarations

Ethical approval This is an original article that did not use other information that requires ethical approval.

Consent to participate All the authors participated in this article.

Consent for publication Authors understand that the text and any pictures or videos published in the article will be used only in educational publications intended for professionals or if the publication or product is published on an open access basis, we understand that it will be freely available on the internet and may be seen by the general public.

Competing interests The authors declare no competing interests.

References

Ahmad Z, Kaario O, Qiang C, Larmi M (2021) Effect of pilot fuel properties on lean dual-fuel combustion and emission characteristics in a heavy-duty engine. Appl Energy 282:116134

Alsudani FT, Saeed AN, Ali NS, Majdi HS, Salih HG, Albayati TM, Saady NMC, Shakor ZM (2023) Fisher-Tropsch synthesis for conversion of methane into liquid hydrocarbons through gas-to-liquids (GTL) process: a review. Methane 2:24–43

Alves CA, Soares M, Figueiredo D, Oliveira H (2023) Effects of particle-bound polycyclic aromatic hydrocarbons and plasticisers from different traffic sources on the human alveolar epithelial cell line A549. Atmos Environ 303:119736

Armas O, García-Contreras R, Ramos Á (2013) Impact of alternative fuels on performance and pollutant emissions of a light duty engine tested under the new European driving cycle. Appl Energy 107:183–190

Bassiony M, Ibrahim A, El-Kassaby M (2016) An experimental study on the effect of using gas-to-liquid (GTL) fuel on diesel engine performance and emissions. Alex Eng J 55:2115–2124

Chaudhary A, Panchal SH, Surana A, Sreekanth M, Ismail S, Feroskhan M (2022) Performance, emission and combustion characteristics of various biodiesel blends. J Therm Anal Calorim 147(3):2455–2479

Chauhan BS, Kumar N, Cho HM (2012) A study on the performance and emission of a diesel engine fueled with Jatropha biodiesel oil and its blends. Energy 37:616–622

Choi K, Park S, Roh HG, Lee CS (2019) Combustion and emission reduction characteristics of GTL-biodiesel fuel in a single-cylinder diesel engine. Energies 12:2201

Gao J, Chen H, Liu Y, Li Y, Li T, Tu R, Liang B, Ma C (2021) The effect of after-treatment techniques on the correlations between driving behaviours and NOx emissions of passenger cars. J Clean Prod 288:125647

García A, Monsalve-Serrano J, Sari R, Dimitrakopoulos N, Tunér M, Tunestål P (2019) Performance and emissions of a series hybrid vehicle powered by a gasoline partially premixed combustion engine. Appl Therm Eng 150:564–575

Ge JC, Wu G, Yoo B-O, Choi NJ (2022) Effect of injection timing on combustion, emission and particle morphology of an old diesel engine fueled with ternary blends at low idling operations. Energy 253:124150

Gundoshmian TM, Heidari-Maleni A, Jahanbakhshi A (2021) Evaluation of performance and emission characteristics of a CI engine using functional multi-walled carbon nanotubes (MWCNTs-COOH) additives in biodiesel-diesel blends. Fuel 287:119525

Hao B, Song C, Lv G, Li B, Liu X, Wang K, Liu Y (2014) Evaluation of the reduction in carbonyl emissions from a diesel engine using Fischer-Tropsch fuel synthesized from coal. Fuel 133:115–122

Huang J, Xiao H, Yang X, Guo F, Hu X (2020) Effects of methanol blending on combustion characteristics and various emissions of a diesel engine fueled with soybean biodiesel. Fuel 282:118734

Işik MZ (2021) Comparative experimental investigation on the effects of heavy alcohols-safflower biodiesel blends on combustion, performance and emissions in a power generator diesel engine. Appli Therm Eng 184:116142

Jin C, Mao B, Dong F, Liu X, Yang Y, Chen P, Zheng Z (2018) Effects of indirect and direct coal-to-liquid fuel on combustion, performance, and emissions in a six-cylinder heavy-duty diesel engine. J Energy Eng 144(3):04018024

Joerger V, Pryor S (2018) Ultrafine particle number concentrations and size distributions around an elevated highway viaduct. Atmos Pollut Res 9:714–722

Kim HY, Ge JC, Choi NJ (2018) Application of palm oil biodiesel blends under idle operating conditions in a common-rail direct-injection diesel engine. Appl Sci 8:2665

Koay LK, Sah MJM, bin Othman R (2019) Comparative study of fuel consumption, acceleration and emission for road vehicle using LPG or gasoline. Adv Struct Mater 102:77–87

Krecl P, Johansson C, Targino AC, Ström J, Burman L (2017) Trends in black carbon and size-resolved particle number concentrations and vehicle emission factors under real-world conditions. Atmos Environ 165:155–168

Liu Y, Tan J (2020) Green traffic-oriented heavy-duty vehicle emission characteristics of China VI based on portable emission measurement systems. IEEE Access 8:106639–106647

Lou D, Qi B, Zhang Y, Fang L (2023) Research on the emission characteristics of a passenger car powered by ethanol, methanol, and liquefied petroleum gas under real-world running conditions. J Energy Res Technol 145:042303

Lü X, Wu Y, Lian J, Zhang Y, Chen C, Wang P, Meng L (2020) Energy management of hybrid electric vehicles: a review of energy optimization of fuel cell hybrid power system based on genetic algorithm. Energy Convers Manag 205:112474

Mei D, Zuo L, Zhang Q, Gu M, Yuan Y, Wang J (2020) Assessment on combustion and emissions of diesel engine fueled with partially hydrogenated biodiesel. J Energy Eng 146:04019038

Miao X, Zhang X, Wang C, Li J, Zhao J, Qu L, Liu Y, Qi S, Li H, Fu M (2024) Effects of fuel and driving conditions on particle number emissions of China-VI gasoline vehicles: based on corrections to test results. Environ Monit Assess 196:591

Prabhu L, Shenbagaraman S, Anbarasu A, Muniappan A, Suthan R, Veza I (2023) Prediction of the engine performance and emission characteristics of Glycine max biodiesel blends with nanoadditives and hydrogen. J Energy Res Technol 145:112701

Prabu A (2018) Engine characteristic studies by application of antioxidants and nanoparticles as additives in biodiesel diesel blends. J Energy Res Technol 140:082203

Praveenkumar T, Rath B, Devanesan S, Alsahi MS, Jhanani G, Gemede HF, Solowski G, Daniel F (2023) Performance and emission characteristics for karanja biodiesel blends assisted with green hydrogen fuel and nanoparticles. J Energy Res Technol 145(11):112702

Ramos Á, García-Contreras R, Armas O (2016) Performance, combustion timing and emissions from a light duty vehicle at different altitudes fueled with animal fat biodiesel, GTL and diesel fuels. Appl Energy 182:507–517

Rao A, Liu Y, Ma F (2023) Numerical simulation of nitric oxide (NO) emission for HCNG fueled SI engine by Zeldovich', prompt (HCN) and nitrous oxide (N2O) mechanisms along with the error reduction novel sub-models and their classification through machine learning algorithms. Fuel 333:126320

Ravaglioli V, Bussi C (2019) Model-based pre-ignition diagnostics in a race car application. Energies 12:2277

Soriano JA, Garcia-Contreras R, Leiva-Candia D, Soto F (2018) Influence on performance and emissions of an automotive diesel engine fueled with biodiesel and paraffinic fuels: GTL and biojet fuel farnesane. Energy Fuels 32:5125–5133

Tan D, Wang Y, Tan J, Li J, Wang C, Ge Y (2024) Influence of ambient temperature on the CO2 emitted of light-duty vehicle. J Environ Sci 140:59–68

Tang G, Wang S, Du B, Cui L, Huang Y, Xiao W (2022) Study on pollutant emission characteristics of different types of diesel vehicles during actual road cold start. Sci Total Environ 823:153598

Tian M, He L, Peng D, Fu M, Ma S, Mu J, Yu Q, Wang J, Yin H, Wang J (2024) Characterizing NOx emissions from diesel trucks with tampered aftertreatment systems and its implications for identifying high emitters. Sci Total Environ 917:170378

Tong Q, Chen H, He J, Su X, Wei Z, Sun F, Xu H, Wang F (2021) Experimental studies of combustion and emission characteristics of diesel engine fueled with diesel/cyclopentanone blend. Energy Rep 7:6756–6768

Verma P, Stevanovic S, Zare A, Dwivedi G, Van Chu T, Davidson M, Rainey T, Brown RJ, Ristovski ZD (2019) An overview of the influence of biodiesel, alcohols, and various oxygenated additives on the particulate matter emissions from diesel engines. Energies 12:1987

Verma S, Kumar K, Das LM, Kaushik SC (2020) Effect of hydrogen enrichment strategy on performance and emission features of biodiesel-biogas dual fuel engine using simulation and experimental analyses. J Energy Resour Technol 143(9)

Verma S, Kumar K, Das L, Kaushik S (2021a) Effect of hydrogen enrichment strategy on performance and emission features of biodiesel-biogas dual fuel engine using simulation and experimental analyses. J Energy Res Technol 143:092301

Verma TN, Shrivastava P, Rajak U, Dwivedi G, Jain S, Zare A, Shukla AK, Verma P (2021b) A comprehensive review of the influence of physicochemical properties of biodiesel on combustion characteristics, engine performance and emissions. J Traffic Transp Eng (english Edition) 8:510–533

Wei S, Ding T, Zhang S, Tao P, Chen J (2020) Analysis of vehicle CO and NOx road emissions test based on PEMS. Energy Sources, Part A: Recover Util Environ Eff 1–15. https://doi.org/10.1080/15567036.2020.1781300

Yang D, Zhang S, Niu T, Wang Y, Xu H, Zhang KM, Wu Y (2019) High-resolution mapping of vehicle emissions of atmospheric pollutants based on large-scale, real-world traffic datasets. Atmos Chem Phys 19:8831–8843

Yuan H, Tsukuda T, Yang Y, Shibata G, Kobashi Y, Ogawa H (2022) Effects of chemical compositions and cetane number of Fischer-Tropsch fuels on diesel engine performance. Energies 15(11):4047

Zhang G, Qiao X, Miao X, Hong J, Zheng J (2013) Effect of coal to liquid fuel on combustion and emission in a heavy-duty diesel engine. Proc Inst Mech Eng Part D: J Automob Eng 227:481–489

Zhang Y, Zhao K, Lou D, Fang L (2022) Study on the real-world emission characteristics of gaseous and particulate pollutants from an inland ship using a portable emission measurement system. Mar Pollut Bull 184:114205

Zhang Y, Lou D, Tan P, Hu Z, Fang L (2023) Effect of catalyzed diesel particulate filter and its catalyst loading on emission characteristics of a non-road diesel engine. J Environ Sci 126:794–805

Zhao J, Ma F, Xiong X, Deng J, Wang L, Naeve N, Zhao S (2013) Effects of compression ratio on the combustion and emission of a hydrogen enriched natural gas engine under different excess air ratio. Energy 59:658–665

Zheng L, Singh P, Cronly J, Ubogu EA, Ahmed I, Ling C, Zhang Y, Khandelwal B (2021) Impact of aromatic structures and content in formulated fuel for jet engine applications on particulate matter emissions. J Energy Res Technol 143:122301